DEUTSCHES ELEKTRONEN – SYNCHROTRON

DESY 92–159
NIKHEF-H/92-15
November 1992

The ZEUS Uranium Calorimeter: Main Characteristics and First Operating Experience

R. Yoshida

NIKHEF-H, Amsterdam, The Netherlands

ISSN 0418-9833

NOTKESTRASSE 85 · D-2000 HAMBURG 52

To be sure that your preprints are promptly included in the
HIGH ENERGY PHYSICS INDEX,
send them to (if possible by air mail):

DESY Bibliothek Notkestraße 85 W-2000 Hamburg 52 Germany	DESY-IfH Bibliothek Platanenallee 6 O-1615 Zeuthen Germany

DESY 92-159
NIKHEF-H/92-15
November 1992

ISSN 0418-9833

The ZEUS Uranium Calorimeter: Main Characteristics and First Operating Experience*

R. Yoshida
NIKHEF-H
P.O. Box 41882, NL-1009 DB, Amsterdam, The Netherlands

for the ZEUS Calorimeter Group

Abstract

The uranium-scintillator calorimeter of the ZEUS experiment in the HERA electron proton collider at DESY in Hamburg, Germany, is described. It covers 99.8% of the solid angle, has an energy resolution $35\%/\sqrt{E}$ for single hadrons and jets, and $17.5\%/\sqrt{E}$ for electrons. e/h is 1 within 2% in the energy range of 2 to 100 GeV. Test beam results show that an intercalibration at the 1% level is achievable using uranium radioactivity. The calorimeter was commissioned in April, 1992, and has been taking data since May, 1992. Main characteristics of the calorimeter construction, readout, and trigger are reviewed. Experience from the first data taking period, including results on noise, stability of calibration, background from HERA accelerator, and performance of the calorimeter trigger is discussed.

*Presented at the III International Conference on Calorimetry in High Energy Physics, Corpus Christi, Sep.29–Oct.2 1992.

1 Introduction

The ZEUS experiment at the HERA electron proton collider at DESY in Hamburg, Germany, has been taking data since May, 1992. The aim of this presentation is, first, to give a review of the ZEUS uranium calorimeter system and, second, to report on the performance of the calorimeter in the first data taking period, from May 1992 to the present.

The HERA e-p collider has been already covered in this conference.[1] Some of the design parameters of this machine are listed in table 1.

The ZEUS detector is shown in figure 1. Charged particles are tracked by the inner tracking detectors, consisting of a vertex detector, a central tracking detector (consisting of cylindrical drift chamber layers), planar drift chambers in the forward and rear directions, and transition radiation detectors in the forward direction.

The thin (1 X_0) superconducting solenoid surrounding the inner tracking detector produces an axial magnetic field of 1.42 T. The uranium calorimeter encloses the solenoid and the inner tracking detectors. The magnetized iron yoke surrounding the calorimeter is instrumented as a backing calorimeter and muon detector. In the forward direction, iron toroids and tracking chambers reinforce muon detection. Downstream of the main detector in the proton direction are six measuring stations installed in the proton ring for detecting forward scattered protons. Close to the beamline upstream of the main detector, photon and electron detectors are installed to measure the luminosity and to detect electrons scattered at small angles.

A main physics topic at HERA is the measurement of proton structure function through Deep Inelastic Scattering (DIS), figure 2. The measurable quantities for the neutral current processes are the energy and angle of the scattered electron, and those of the current jet. For the charged current process, the only available quantities are those of the current jet.

Other topics of interest include low-x physics, photoproduction, heavy quark spectroscopy, and the search for exotics.

The following, then, are the requirements for calorimetry at HERA.

- Hermeticity.
- Very good jet energy resolution.
- Good position resolution.
- Fast response to avoid pile up at bunch crossing rate of 10 MHz.
- Triggering and readout capable of avoiding long deadtime at above rate.
- Timing resolution in nanosecond range for cosmic and beam gas rejection.
- Wide dynamic range to handle up to 400 GeV showers in the proton direction.
- Calibration good to 1% level.
- Uniform response.

- Good electron hadron separation.
- Radiation hardness to tolerate 20 rad/day, close to the beampipe.

The ZEUS decision has been to build a uranium-scintillator calorimeter with full intrinsic compensation. It has been demonstrated through many tests of prototypes and final modules, Monte Carlo studies, and, finally, through the performance of the calorimeter in the ZEUS experiment, that the advantages of this calorimetry technique can be fully exploited.

2 Calorimeter System Design

2.1 Calorimeter Structure

The basic structure of the calorimeter is plates of depleted uranium, clad in stainless steel foil, interleaved with scintillator tiles. Each layer is approximately 1 X_0 thick. Extremely strict quality control has been enforced, mechanical tolerances being typically better than 1%. The thickness ratio of 3.3 mm U to 2.6 mm scintillator, chosen to give $e/h = 1$, is given by predictions based on understanding of the compensation mechanism achieved through many Monte Carlo studies and prototype tests.[2-9] For the details of construction the reader is referred to Ref. 10, 11, and 12, for the optical components Ref. 13, 14, 15, and 16.

The calorimeter tower structure is shown in figure 3. Towers make up modules, figure 4, and modules are stacked to make up the calorimeter, figure 1. The calorimeter is mechanically divided into 3 parts. The forward, barrel and rear section are called, respectively FCAL, BCAL, and RCAL. Forward and rear are defined with respect to the proton direction. The coverage is 99.8% in the forward hemisphere and 99.5% in the backward hemisphere. The sandwich which forms a tower is read out on both sides by wavelength shifter bars (WLS). A tower is longtitudinally segmented into an electromagnetic subtower(EMC), of 1 λ (25 X_0), and two (one for the rear section) hadronic subtowers(HAC1 and HAC2), of 3 λ each (2 λ for the barrel section). Each subtower, called a cell, is read out by 2 photomultiplier tubes(PMT's), one on either side. The typical transverse dimensions of a HAC is 20 cm by 20 cm. EMC's are further segmented to 5 cm by 20 cm in the towers in the forward and barrel sections, and to 10 cm by 20 cm in the rear section.

2.2 Readout[17]

2.2.1 Analog Cards

The 96 ns beam crossing times at HERA, an order of magnitude shorter than at other existing colliders, require novel approaches in signal processing. A trigger capable of cutting the rate to 1 kHz requires at least a few μs to arrive at a decision. This means the data from almost 12k channels must be buffered for this length of time. The overview of the readout scheme is shown in figure 5.

The readout electronics mounted on the detector are called Analog Cards. The signals from the PMT are split to low and high gains to allow for a dynamic range of 1 to 40000. The signals are then shaped to approximate a triangle to allow sampling both on the raising and falling edge and to give an effective gate width of 130 ns required for full compensation.

The resulting signal is sampled at the HERA frequency of 10 MHz, and the result is stored in an analog pipeline, also clocked at 10 MHz. The pipeline is a custom made IC working on the switched capacitor principle. It has 58 cells, giving a storing time of 5.6 μs.

Another custom IC on the Analog Cards is the buffer/multiplexer chip. The buffer is needed to avoid long deadtime due to pipelines being read while samples are digitized, and works on the same principle as the pipeline chips. Signals from 6 PMT's are multiplexed, and sent over 60 m of cable to the digitizing electronics.

2.2.2 Digital Cards

The digitizing electronics reside in VME crates in the electronics area of the experiment. These cards, called Digital Cards, have built in digital signal processors (DSP's), as well as 12-bit ADC's with conversion time of 1.75 μs per sample. All constants related to the electronics in the Analog Cards, and the ADC's, are generated in special calibration runs and are downloaded onto the Digital Cards. DSP's provide as output energy and time of signal arrival with respect to the 10 MHz HERA clock for each PMT, reconstructed from the samples, with all corrections applied.

2.2.3 Transputer Based Readout[20]

Transputers are microprocessors with large connectivity. Each transputer has 4 bidirectional processor to processor links with transfer rate of up to 2.5 Mbytes/s. The transputer was especially designed for the parallel processing language OCCAM, and this makes writing an efficient parallel processing code relatively easy.

A VME module with 2 transputers (2TP modules) were designed especially for ZEUS. These modules reside on the same VME bus as the Digital Cards. One of the transputers of the 2TP module is designated for (second level) trigger processing and the other for readout. When the data from the DSP's are available, the Digital Cards signal the readout transputer to read out a subset of the data (called second level trigger data) and the readout transputer places the data in a memory shared with the trigger transputer. The trigger transputer is a part of the second level trigger network to be described below. When a positive second level trigger decision is received by the readout transputer, it reads out the main part of the data and sends it to the event builder system which assembles complete events from data of all of the ZEUS components.

2.3 Trigger

2.3.1 Calorimeter First Level Trigger(CFLT)[18]

Because the 96 ns bunch spacing is much shorter than the trigger processing time, ZEUS first level trigger(FLT) is designed to process new data every 96 ns and produce a decision at this rate. The design accept rate of the FLT is around 1 kHz at full luminosity.

The Analog Card provides 5% of the PMT signal to the front end trigger electronics where signals from several cells are summed together. These signals are then integrated, clipped and sent 60 m to the digitizing electronics outside the detector. The signals are digitized and tested against thresholds, summed further by trigger towers, and processed, using look up tables, to produce information on total E, transverse E, longititudinal E, and isolated leptons for each of the 16 trigger regions. The trigger towers are defined in such a way as to have a projective geometry and are different from the towers described in 2.1. Eventually all information is gathered in the Calorimeter First Level Trigger Processor (CFLTP)[19], which determines global calorimeter quantities, and provides information on clusters, and likelihood of the data being from a beam-gas event.

CFLTP sends the information to Global First Level trigger (GFLT) which gathers information from all components and issues an accept or a reject.

2.3.2 Calorimeter Second Level Trigger(CSLT)[20,21] and the Third Level Trigger(TLT)[23]

The 16 event output buffer in the Digital Cards, at the 1 kHz design rate of the first level trigger, allows order 5 ms for the average latency of the second level trigger decision. This time scale allows the use of microprocessors. The ZEUS system exploits the large connectivity of transputers to process a subset of the calorimeter readout data to do a more sophisticated analysis of energy deposit pattern and timing for further rejection of beam-gas, beam halo muons, cosmics, and other background events. The CSLT information is sent to the ZEUS Global Second Level Trigger[22], which receives second level trigger data from all components and generates a decision. The positive second level trigger decision rate is expected to be around 100 Hz at full luminosity. Complete data for events that passed the second level trigger are assembled and sent to the Third Level Trigger (TLT).

The TLT is a farm of Silicon Graphics work stations, which runs a subset of offline reconstruction software. Here final selection for the physics events are made. The expected rate of output for the TLT is a few Hz.

The readout-trigger system is designed to run with a few percent deadtime at full luminosity.

2.4 Calibration Tools

2.4.1 Uranium Radioactivity

The "noise" in the calorimeter due to the decay of ^{238}U (UNO) provides a very stable calibration signal. There is 1 decay every 1 ns in even the smallest cells. A single reading of the integration of this signal for 20 ms corresponds to an accuracy better than 1%. This current (I_{uno}) is directly proportional to the gain of the channel being measured, up to and including the PMT.

At beam and cosmic tests, all PMT gains were set so that I_{uno} was within 1% of some nominal value, which varies according to the size of cell. The reconstructed charge of each channel was multiplied by the factor $I_{uno}^{nominal}/I_{uno}^{measured}$.

In the test of the FCAL prototype, which has identical construction as the final modules, a measurement of UNO was made every 2 hours for a period of 30 days. The results for 1 channel are shown in figure 6. The short time variation (δ) is defined as the difference between 2 consecutive measurements. The long term variation (Δ) is defined to be the largest variation in the test period. The results from this type of tests for large number of channels showed that a UNO taken at 8 hour intervals is sufficient to monitor PMT gains to within 0.5%.

The intercalibration of the cells from the setting of PMT gains by the I_{uno} setting were examined in these tests. As an example, figure 7 shows the spread of the reconstructed charge for cosmic muons in FCAL HAC1's. The plot has one entry per cell measured, and the spread is less than 1%. The cell to cell, and module to module response measured with electrons, hadrons, and muons are in the range of 1 to 1.5%.

The absolute energy scale was measured in test beams, where precise beam momentum measurements were available. The I_{uno} stability and uniformity over modules, allow the transport of this calibration from the test beam to the experiment, provided the modules are mechanically stable.

2.4.2 Electronics Calibration

Programmable precision DC voltage (calibrated to 0.1%) and charge injection (calibrated to 0.2%) built into the Analog Cards are used to measure gains and linearities, absolute charge scale, and low/high gain ratio of the electronics. Trigger electronics is also calibrated with the charge injection of the Analog cards. The effect on the resolution of the calorimeter due to electronics noise and non-linearity is measured to be very small compared to the contribution from other sources. The stability of electronics calibration in the actual experiment will be dicussed below.

2.4.3 Pulsed Light System

The calorimeter is also equipped with laser and LED light injection system to allow monitoring of PMT performance through photoelectron count, measurement of linearity to energies not accessible through test beam, and calibration of time measurement. The last item plays an important role in triggering at ZEUS which will be discussed below.

2.5 Beam and Cosmic Ray Tests

2.5.1 Summary of Previously Reported Results

Many results from beam and cosmic tests have already been presented and most are now available in literature.[9,11,24-26] In addition, results of the BCAL beam tests at Fermilab will be covered elsewhere in this conference.[27] The following is a summary of results from tests of the final FCAL and RCAL modules, and the FCAL prototype module, which has identical construction as the final modules.

Figure 8 shows the energy resolution for electrons and hadrons for the FCAL prototype. The electron energy resolution for the 10 final modules which were tested at CERN was found to be $17.6\%/\sqrt{E}$ for FCAL, $17.4\%/\sqrt{E}$ for RCAL at an electron energy of 15 GeV, after subtraction of the beam momentum spread.

The e/h ratio measured with the FCAL prototype is shown in figure 9. Calorimeter response was measured to be linear to within 1% for electrons in the range of 15 to 110 GeV, for FCAL EMC's. RCAL and FCAL HACs, which use a different type of PMT showed up to 2% deviation within this range. The latter can be corrected offline.

Nonuniformities at module and tower boundaries was found to have negligible effect for hadron showers. Electron response was checked by scanning across the boundaries with electron beams at various angles of incidence. It was found that the effect at module boundaries are large, where the Cerenkov light produced in the WLS tends to increase the module response. At normal incidence, this effect can be as large as 65%. This problem can be countered by lead sheets inserted between the modules to absorb part of the electromagnetic shower. Figure 10 shows the comparison of uniformity for test beam data with and without lead foil. The optimum thickness of the lead sheet was found from the test beam data, and 2.6 mm lead foils were inserted between modules. In ZEUS, electrons always enter the bounderies at an angle, thus smearing out the effect of the gaps.

2.5.2 Jet Resolution Measurements

Previously unreported measurements of simulated jet energy resolution were made at CERN SPS, using FCAL prototype modules. 50 and 100 GeV pion beams impinged on a thin Be target (0.03 λ). Events with wide angle tracks were vetoed by lead glass walls. The trigger was based on a wall of scintillation counters giving a pulse consistent with greater than 4 minimum ionizing particles.

Figure 11 show the energy resolutions of "jets" compared to those of pions taken at the same apparatus. "Jet" resolution is seen to be better than the pion resolution. The result does not take the fluctuation of energy due to the loss of energy in the target, which degrades the energy resolution, into account.

3 Performance in the First Data Taking Period

3.1 HERA in the First Data Taking Period

In the first data taking period from May to July 1992 the HERA collider ran in a low intensity mode, both proton and electron current being around 1 to 2 mA. Typical luminosity was 1 to $5 \times 10^{28} cm^{-2} s^{-1}$. There were 10 bunches of protons colliding with 10 bunches of electrons. The spacing between the bunches, however, was 96 ns, as designed.

3.2 Energy Measurement

The absolute energy scale was set by adjusting the PMT gain using the uranium current, I_{uno}, according to the scale measured in test beams. Figure 12 shows the energy measured in FCAL and RCAL from beam halo muons. They agree with measurements made with cosmic rays and with test beam muon measurements within 5%. More precise check of the absolute calibration from muons will be available with increased statistics and muon momentum determination from the ZEUS muon detectors. The intercalibration determined from the muon energy deposit in HAC(EMC) cells in FCAL and HAC(EMC) cells in RCAL is better than 1%. Data on the noise in the RCAL is shown in figure 13. Examination of the whole calorimeter shows noise at the level of 8 to 12 MeV from EMC cells, and 14 to 32 MeV in HAC cells. These results are the same as that measured at test beams. This value corresponds to around 200 MeV of noise for towers to be summed together for a typical jet.

The effect of magnetic field has been studied in detail. It is known that light output of scintillators is affected by magnetic field and extensive tests were done. The highest field occurs in RCAL. It is also known that the magnetic field effect in the scintillator is different for UNO and electron signals.[28] This was measured in a test beam and is shown in figure 14. Monte Carlo studies and calculations based on the tests show, however, that in ZEUS configuration the effects cancel, and UNO calibration taken with the field on is good to better than 1% in the worst affected channels.

3.3 Time Measurement

The time resolution of the calorimeter measured with the laser calibration system is around 0.3 ns above a few GeV of deposited energy per cell. This represents the limit of achievable time resolution for the ZEUS calorimeter. Figure 15 shows the time resolution as a function of energy deposition, measured by the laser system. Systematic effects in the time offset meaurement, as well as hadron shower related effect limit the time resolution to about 1 ns.

Figure 16 shows the time resolution for FCAL and RCAL from HERA data. The resolution, which also contains the effect of the proton bunch length, is about 1.5 ns. A cut is applied at energy deposit per cell of 1 GeV and only the cells around the beampipe are used for this measurement. This resolution, as will be discussed in the

section on trigger performance, is adequate for rejecting (proton) upstream beam gas interactions cleanly online if there is enough energy deposit in both FCAL and RCAL.

3.4 Trigger Configuration and Performance

The trigger configuration in the first run period was kept looser and simpler than designed. For the first level trigger, simple thresholds were set per trigger tower, transverse dimension 40 cm by 20 cm, separately for EMC and HAC sections. The thresholds values designed for DIS events is shown in figure 17. Monte Carlo studies showed that this trigger is 98% efficient for neutral current events with $Q^2 > 10\ GeV^2$. This trigger combined with a set of small veto scintillator counters around the beampipe near RCAL, gave a rate of about 5 Hz under the running conditions in the first period of data taking.

CFLT electronics was calibrated before installation. The intercalibration of trigger towers measured after installation is shown in figure 18, and is good to 1%. The absolute energy calibration of the trigger was found to be better than 10%. In the first data taking period, 3% of the trigger towers were not read out due to various hardware problems. The overall efficiency of the trigger is process dependent, but redundancy of the trigger due to the topology of events ensures that effect from miscalibration and non-working channels are small.

Because of the flexible design of the second and third level triggers, algorithms tested in the offline on real data could be implemented first in the third level trigger, where the programming is relatively easy, then moved to the second level trigger. This feature is an essential part of the ZEUS trigger strategy.

A trigger cut introduced in this way was a rejection of proton related background with timing information from the calorimeter. The dominant background at ZEUS comes from protons interacting with beam gas and off momentum protons striking the beam pipe wall, or other objects, in the 100 m straight section before the detector. The time measured in the calorimeter is normalized so that the particles from the e-p interaction point arrives at time 0 at the calorimeters. Particles from interactions of protons upstream of the detector will arrive earlier than particles from e-p collision at RCAL by 10 ns. Moreover, the difference in the time of arrival at FCAL and RCAL, $t_f - t_r$, subtracts out the size of the proton beam, which was much longer than the electron beam for this period, for beam gas events. And t_r is narrow for e-p events, since it depends on the length of the electron beam. Thus plotting the average $t_f - t_r$ versus average t_r for cells with energy deposit over 1 GeV around the beampipe, one obtains a clear separation of peaks from e-p interaction candidates and background as shown in figure 19. About 80% of the beam gas events have measureable time in both FCAL and RCAL and 95% of these events are rejected online using conservative cut values.

Some of the other cuts at higher level triggers either implemented, or under study include, "spark" rejection, where events triggered by cells with large imbalances in the two PMT's are cut away, cosmic ray rejection using tracking information in conjunction with information from BCAL, and clustering algorithms to reject remaining beam related backgrounds.

The readout-trigger system ran without deadtime under normal conditions in the first data taking period.

3.5 Stability of the System

As discussed above, the stability of the absolute calibration is tracked by the UNO measurement. Stability of the UNO was found to be compatible with the measurements made at test beams, discussed in section 2.4.1.

Figure 20 shows the results of charge injection to check the electronics calibration. These runs were taken 9 days after the system was calibrated for the electronic constants, and show that the channel to channel calibration is still good to 0.1%. In the period from April to July, the fraction of single channels not readout because of hardware problems was on average around 2%. However, because of the redundant readout of a cell, and the design that separate the readout paths of the two PMT's reading out the same cell, the fraction of bad cells not read out was on average less than 0.1%. However, an access to the detector of around 8 hours, once every 2 or 3 weeks, for maintenance and repair of readout electronics was required to keep problems down to this level.

3.6 Hadron Electron Separater (HES) Tests

HES is a planned system of silicon diode detectors to be inserted into the calorimeter to aid in hadron rejection. Each diode has dimension 3.3 cm x 3 cm and is to be mounted at 3 X_0 from the face of the calorimeter. HES will cover 10 m^2 surface area in RCAL, and two layers of 9 m^2 in FCAL. BCAL would require 20 m^2 of surface area, and because of the high cost, alternate technologies are under investigation.

Monte Carlo and test data show that the HES system can enhance the hadron rejection by factors of 10 to 20, when electrons are near or in a jet, depending on conditions.

Three of the RCAL modules were equipped with HES for the first running period. This amounted to 2000 channels of readout. Figure 21a shows the hadron and electron signals in HES taken at the CERN test beam. Figure 21b shows the HES response to the electron candidates from a NC DIS event sample, superimposed on the plot is the response to beam halo muons. The whole of RCAL is to be equipped with HES during the winter shutdown '92-'93.

3.7 Radiation Issues

Scintillator, WLS materials and electronics of the calorimeter have been tested for radiation hardness and 35 rad/day has been determined to be the upper limit of acceptable dose. The limiting factor is the CMOS electronics.

The level of radiation dose 10 cm from the beam pipe, the distance of the closest approach of the calorimeter, has been measured during the HERA machine study period from April to December 1991. The study showed that the dose extrapolated to the full design current is at the level of 25 rad/day and up to 240 rad/day under

the sometimes unstable operating conditions of the machine study. The highest doses were observed during beam injection and tuning. The level of radiation dose from the uranium radioactivity is around 3 rad/day.

FCAL and RCAL support structures have been designed with hydraulic systems that move the calorimeters up to 40 cm away from the beampipe. The calorimeters are in the "open" position, away from the beam pipe during injection and tuning of the beams, and are moved to the data taking position only when stable beam conditions have been established.

The radiation dose observed during the first running period is small and dominated by the uranium radioactivity. The highest beam related doses occured in uncontrolled losses of beam in the startup phase of HERA. The measured doses from the beam in this period at the calorimeter typically did not exceed 200 mrads/day.

4 Conclusion

The ZEUS high resolution uranium calorimeter has been installed in the experiment and has been taking data since May, 1992. The performance of the detector in ZEUS is consistent with the performances measured in the lab for various subcomponents, in beam tests, and in cosmic tests.

The absolute calibration has been set using the uranium radioactivity and is believed to be good to 1%. The calibration has been checked, using beam halo muons, to 5%. More precise determination will be available as various ZEUS tracking components come online.

The reliability of the electronics components have been good, but require some access to the detector at regular intervals for repair and maintenance. Damaging radiation from HERA accelerator has been at a negligible level in the first running period.

5 References

1. R. Brinkmann, to be published in *Proceedings of the III International Conference on Calorimetry in High Energy Physics*, Corpus Christi (September 29–October 2, 1992)
2. H. Brückmann *et. al, NIM* **A263** (1988) 136.
3. R. Wigmans, *NIM* **A259** (1987) 389.
4. M. G. Catanesi *et. al., NIM* **A260** (1987) 43.
5. B. Anders *et. al., DESY preprint* 86-105.
6. J. J. Engelen *et. al., NIKHEF-H preprint* 86-18.
7. G. d'Agostini *et. al., NIM* **A274** (1989) 134.
8. G. Drews *et. al., NIM* **A290** (1990) 335.
9. U. Behrens *et. al., NIM* **A289** (1990) 115.
10. M. Derrick, *et. al., NIM* **A309** (1991) 77.
11. A. Andresen *et. al., NIM* **A309** (1991) 101.
12. J. Straver, Ph.D. thesis, University of Amsterdam, (1991).
13. B. G. Bylsma, *et. al., NIM* **A305** (1991) 354.
14. J. Hartmann, *et. al., NIM* **A305** (1991) 366.
15. B. Lu *et. al., NIM* **A313** (1992) 135.
16. T. Ishii *et. al.*, submitted to *NIM*
17. A. Caldwell, *et. al., NIM* **A321** (1992) 352.
18. W.H. Smith, *Proceedings of the Workshop on Triggering and Data Acquisition for Experiments at the Supercollider*, Toronto (January 16–19, 1989).
19. J.W. Dawson *et al., IEEE Transactions on Nuclear Science,* **37** (1990) 2198.
20. L. W. Wiggers and J. C. Vermeulen, *Comp. Phys. Comm.* **57** (1989) 316.
21. S. deJong, Ph.D. thesis, University of Amsterdam, (1990).
22. H. Uijterwaal, Ph.D. thesis, University of Amsterdam, (1992).
23. D. Baily *et. al.*, in *Open Bus Systems '92*, Zürich, (October 1992). and D. Baily *et. al.*, to be published in *Proceedings of the Conference on Computing in High Energy Physics*, Annecy, (September 1992).
24. I. Ambats *et. al., NIM* **A320** (1992) 161.
25. A. Bernstein *et. al.* to be submitted to *NIM.*
26. U. Behrens *et. al.* to be submitted to *NIM.*
27. M. Z. Wang, to be published in *Proceedings of the III International Conference on Calorimetry in High Energy Physics*, Corpus Christi (September 29–October 2, 1992).
28. J. Mainusch *et. al., DESY preprint* 91-027.

Figure 1 The ZEUS apparatus, side view. The uranium calorimeter is labeled FCAL (Forward CAL), BCAL (Barrel CAL), and RCAL (Rear CAL). Forward and rear are defined with respect to the proton beam.

Figure 2 Feynman diagram describing the deep inelastic e-p scattering in the lowest order.

Figure 3 Tower structure of the ZEUS calorimeter. The figure shows a tower of the forward section.

Figure 4 Calorimeter Modules: On the left is a module from the barrel section. On the right, a module from the forward section. The largest forward module is 4.6 m tall and weighs about 12 tons.

Figure 5 An overview of the readout scheme

Figure 6 UNO stability as measured with the FCAL prototype. For definition of δ and Δ, see text.

Figure 7 Shown is the most probable value of the charge distribution for each cell in the cosmic muon measurement. The sigma of the distribution, at about 0.8%, shows the goodness of the calibration with uranium current only.

Figure 8 Energy resolution for electrons and hadrons as measured with the FCAL prototype is plotted as a function of kinetic energy, E_{kin}, in logarithmic scale. The data for hadron measurement below 10 GeV include protons and pions, above 10 GeV are pions only. Hadron resolution improves below 2 GeV as fraction of energy loss to ionization increases.

Figure 9 e/h ratio as measured in the FCAL prototype. Same data set as in figure (8). e/h ratio deteriorates below 2 GeV and begins to approach the value of e/mip, where mip is the minimum ionizing particle response.

Figure 10 Average shift from uniform response due to the nonuniformity at a module boundary, averaged over a region of 20 cm around this boundary, plotted as a function of incidence angle, and for different thicknesses of lead. The angles corresponding to the boundary(crack) in FCAL as seen from the interaction point are marked. In the final choice of the lead thickness, shift, rms, and mean square deviation from uniformity of the electron response across the boundary was taken into account.

Figure 11 Fractional difference in resolution of jets and pions

Figure 12 Calorimeter response to beam halo muons in ZEUS. The data are for FCAL HAC1 and RCAL HAC1 sections. The most probable value of the Moyal function fit for these sections are respectively, 1.094 and 1.093 GeV. The EMC section responses also agree to better than 1%.

Figure 13 RCAL noise as measured by empty triggers are plotted. There is one entry per channel. Energy scale is MeV. The lowest peak is for channels with high voltage to the PMT's turned off and shows the level of electronics noise. The second highest peak is for the EMC's and the third for the HAC's. The noise is dominated by UNO and therefore is proportional to the surface area of the uranium seen by the scintillators in the cell.

Figure 14 Magnetic field effects on UNO and beam signals. This data compares the change in the light output of the scintillator material used in ZEUS calorimeter, for UNO and for 2 and 6 GeV electron beams as a function of magnetic field.

Figure 15 Time resolution as a function of energy deposit, in the RCAL, per channel, as measured by laser. The dotted line represents the time jitter of the laser signal as measured by a TDC, and should be subtracted in quadrature. The deterioration of resolution observed around 9 GeV is due to the change from low to high gain digitization. The time scale is in nanoseconds.

Figure 16 The FCAL and RCAL times for beam gas events. A 1 GeV energy deposit per cell is required. Only a few cells in the calorimter, around the beam pipe, is used for this measurement. The width of the time resolution also includes the effect of the proton bunch length.

Figure 17 Trigger thresholds for the first running period. In RCAL, the threshold for the dark region was 10 GeV per trigger tower (transverse dimension 20 cm by 40 cm), and 2.5 GeV for the light region, for the EMC sections. All regions of BCAL also had the threshold of 2.5 GeV for EMC sections. BCAL and RCAL did not trigger on HAC sections. In FCAL, the dark region had threshold 50 GeV and 70 GeV for EMC's and HAC's respectively, the shaded region had 20 and 25 GeV, the light section 10 and 10 GeV. Lines indicate the cell structures.

Figure 18 CFLT calibration. Charge injectors on Analog Cards are fired and the energy seen by CFLT and the readout are compared.

Figure 19 Average $t_f - t_r$ vs. average t_r for e-p data. Only cells with greater than 1 GeV energy deposit is used. Note that the vertical axis is in logarithmic scale. The small peak is the e-p interaction candidates.

Figure 20 Charge injection reconstructed values for BCAL and RCAL. There is one entry per channel.

Figure 21 HES response in test beam, a) and in ZEUS b), plotted in terms of mip's. The beam data is for 9 GeV electrons and pions. ZEUS data are for electron candidates from DIS neutral current event candidates and beam halo muons, barely visible at 1 mip.

	e-ring	p-ring
Nominal Energy	30 GeV	820 GeV
Bunches	210	210
Number of particles	0.8×10^{13}	2.1×10^{13}
Time between bunch crossings	96 ns	
Luminosity	$1.5 \times 10^{31} cm^{-2} s^{-1}$	

Table 1: Some HERA design parameters

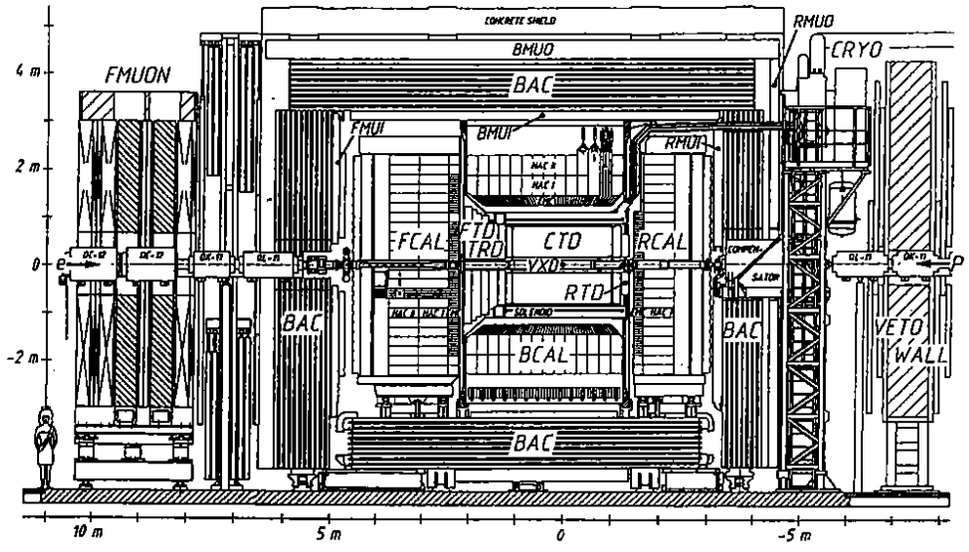

Figure 1

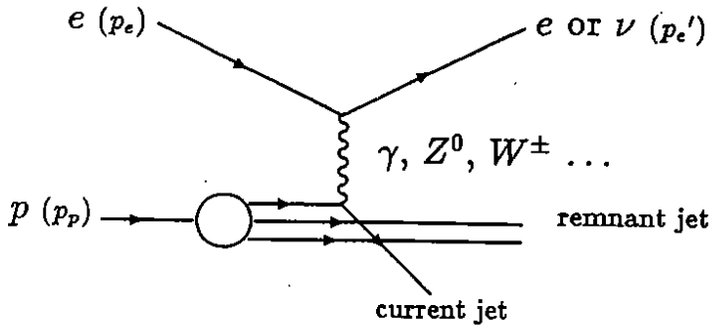

Figure 2

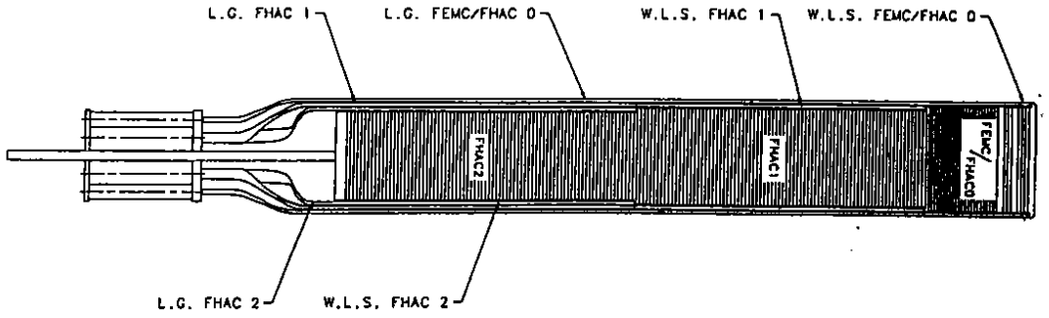

Figure 3

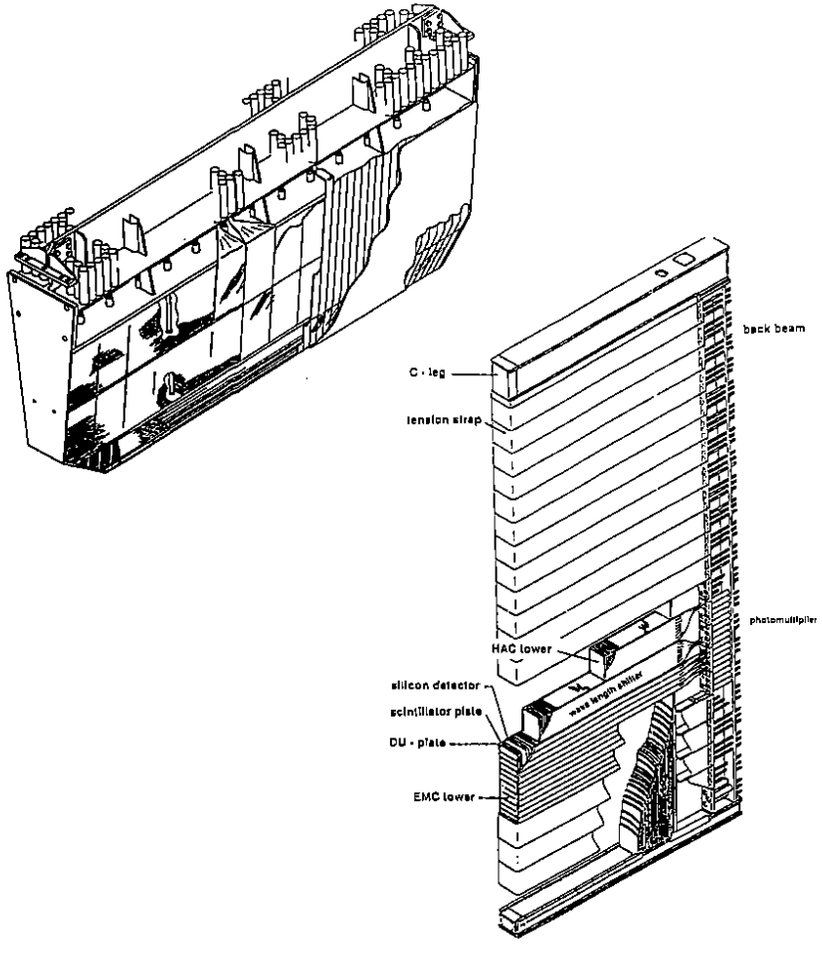

Figure 4

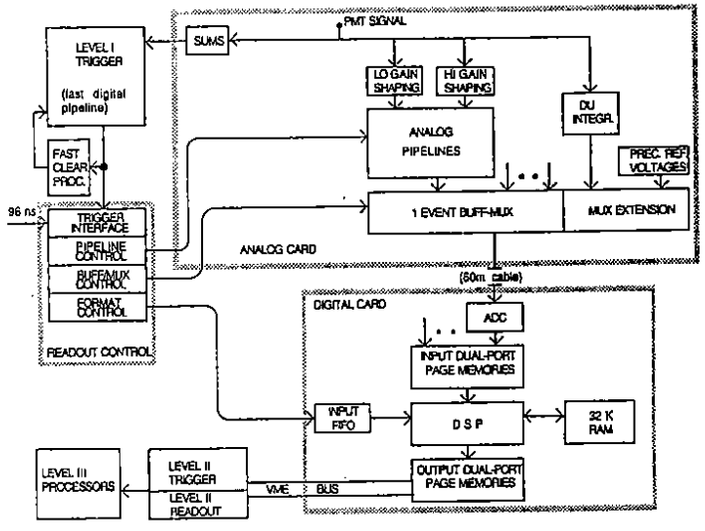

Figure 5

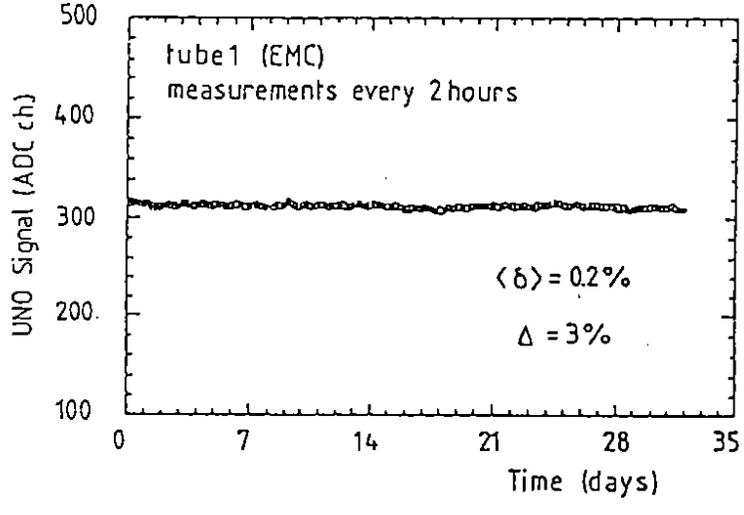

Figure 6

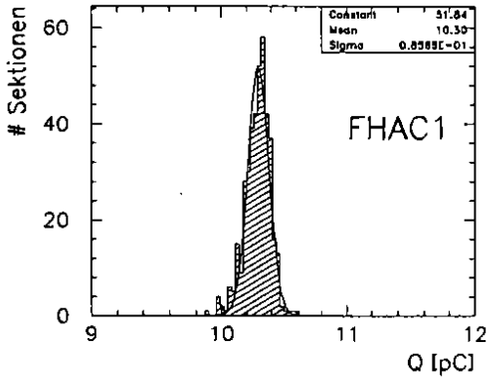

Figure 7

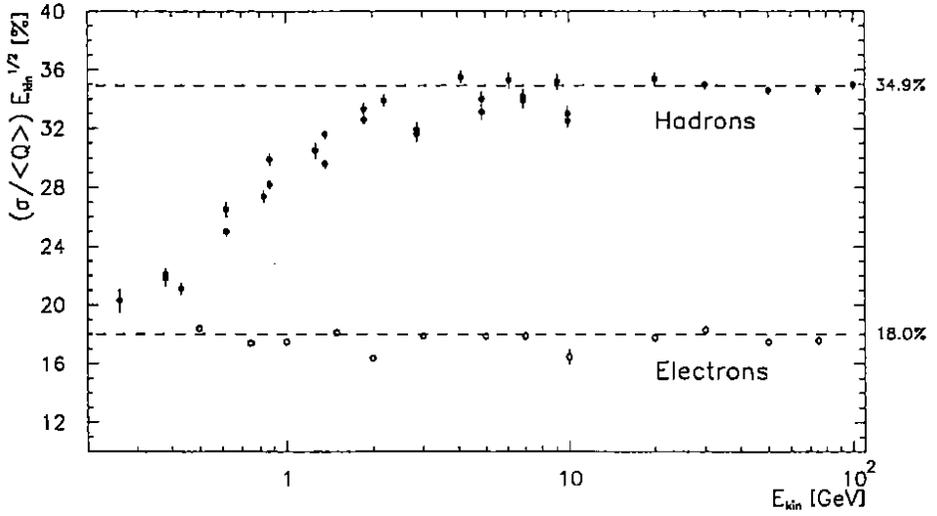

Figure 8

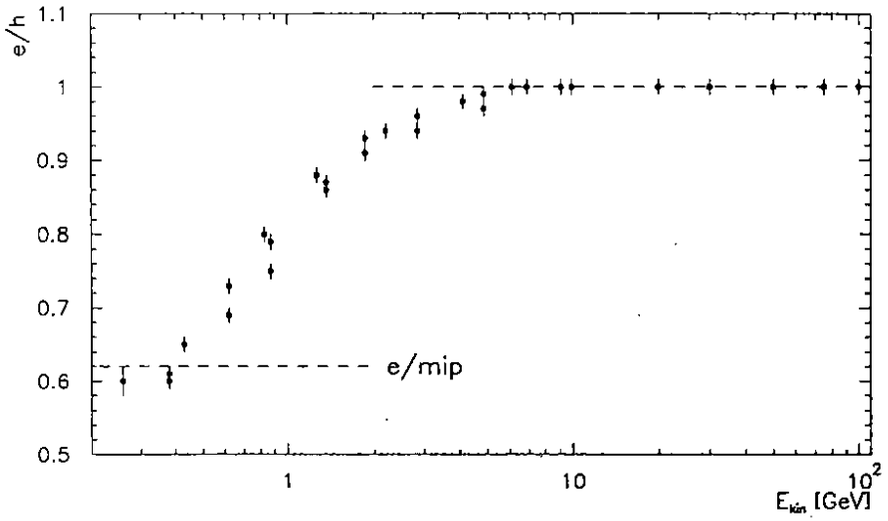

Figure 9

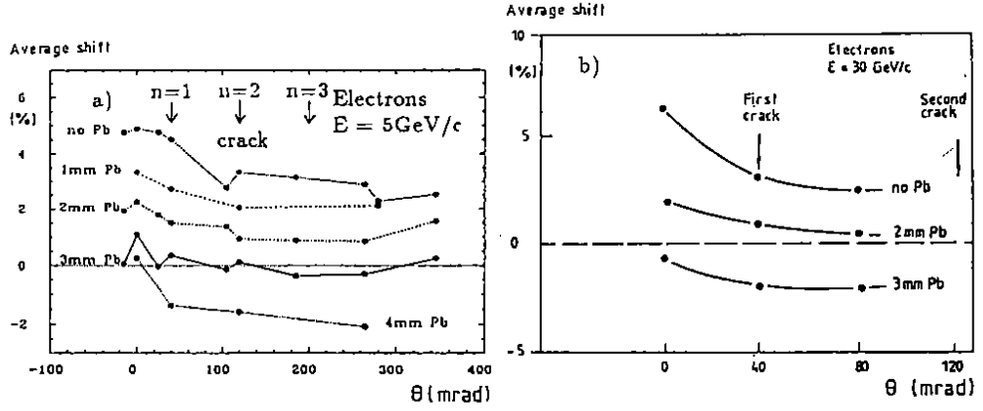

Figure 10

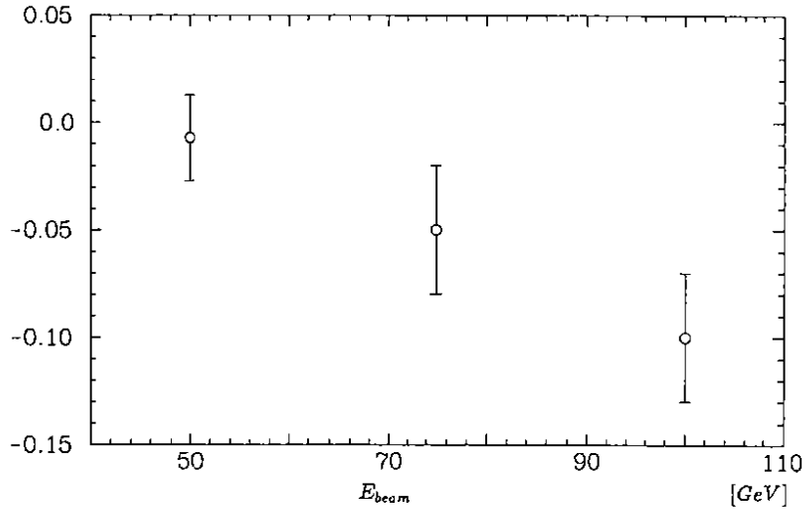

Figure 11

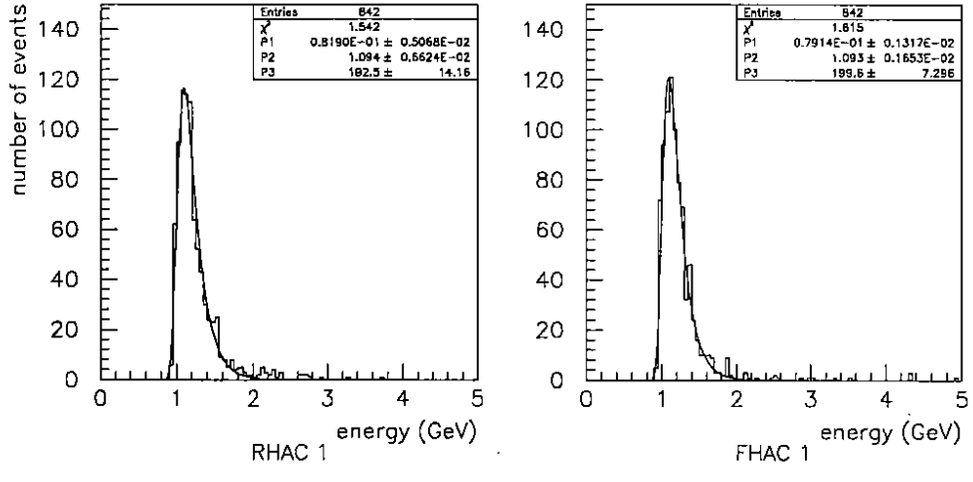

Figure 12

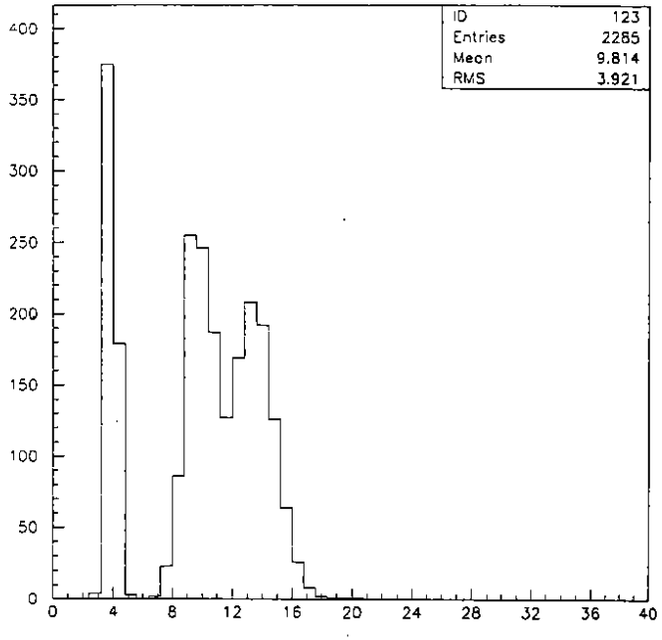

Figure 13

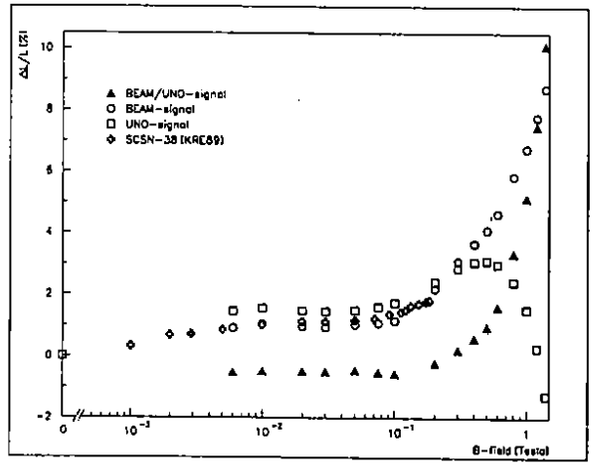

Figure 14

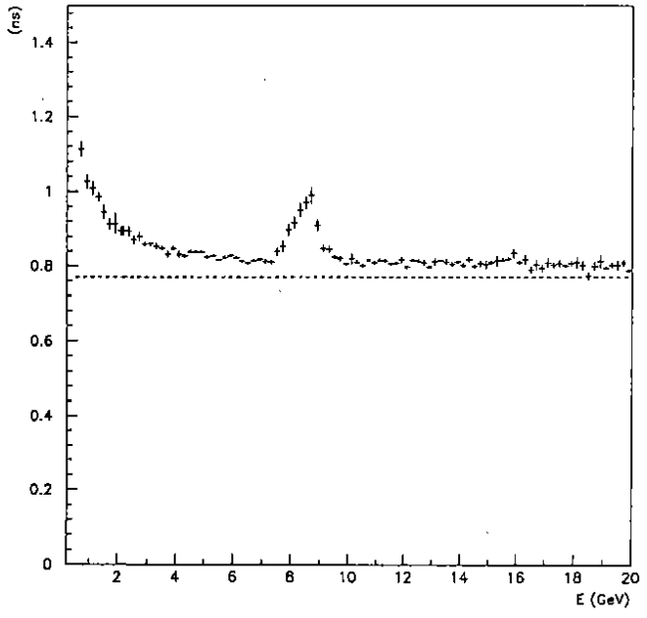

Figure 15

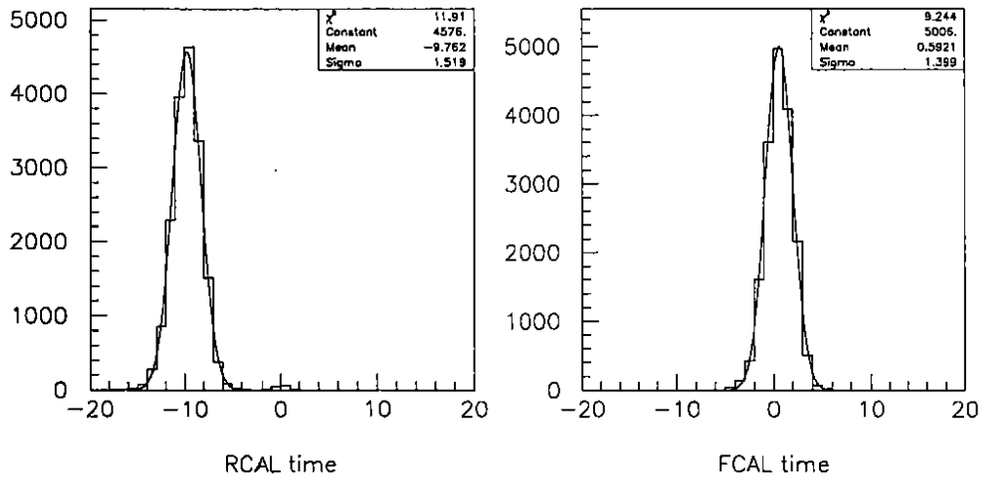

Figure 16

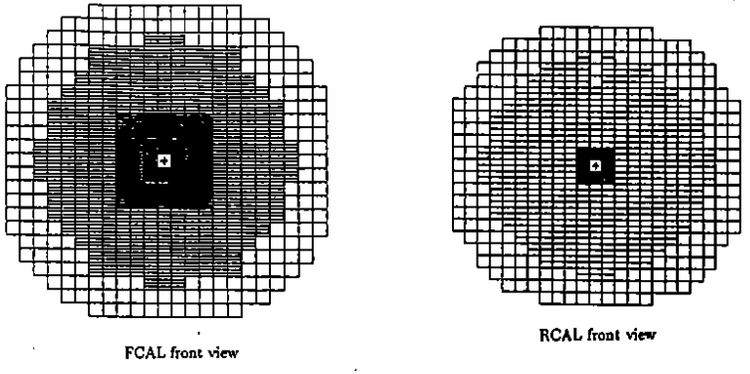

Figure 17

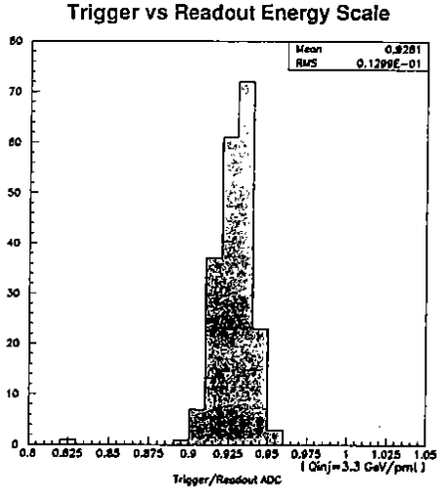

Figure 18

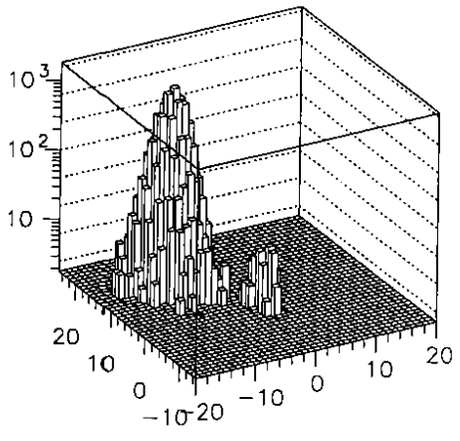

Figure 19

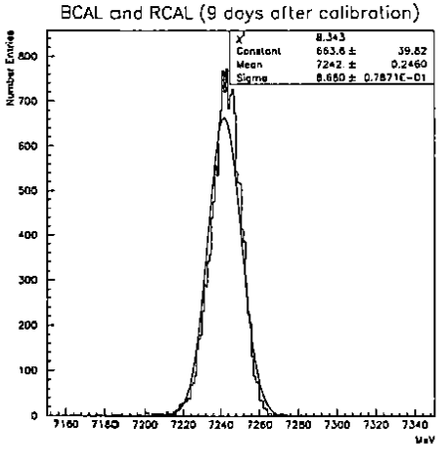

Figure 20

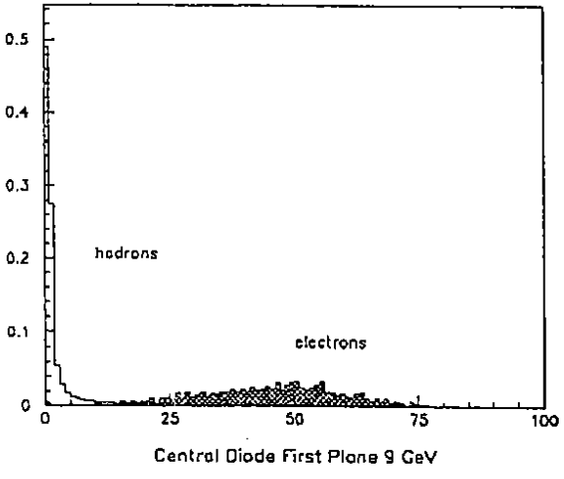

Figure 21a

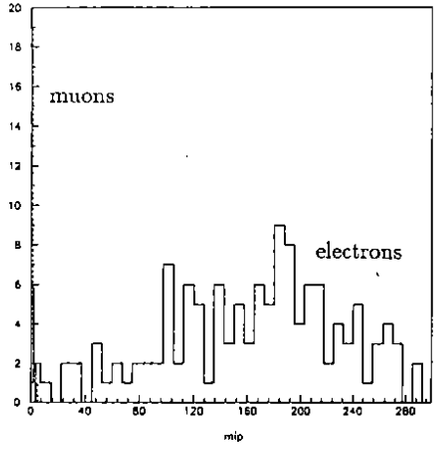

Figure 21b